Hexaphyrin-cyclodextrin hybrids: Getting larger, getting confused

François Robert, Bernard Boitrel, Mickaël Ménand, Stéphane Le Gac

Hexaphyrin-Cyclodextrin Hybrids: Getting Larger, Getting Confused

François Robert,[a] Bernard Boitrel,[a] Mickaël Ménand,[b,*] and Stéphane Le Gac [a,*]

a Univ Rennes, CNRS, ISCR (Institut des Sciences Chimiques de Rennes) – UMR 6226, Rennes F-35000, France.

b Sorbonne Université, CNRS, Institut Parisien de Chimie Moléculaire (IPCM) – UMR 8232, 4 place Jussieu, 75005 Paris (France)

Received date (to be automatically inserted after your manuscript is submitted)
Accepted date (to be automatically inserted after your manuscript is accepted)

ABSTRACT: The diversity of hexaphyrin-cyclodextrin hybrids (HCD), previously formed from the covalent assembly of regular hexaphyrin and α-cyclodextrin subunits, has been increased following two main directions: enlarging the confined space provided by the cyclodextrin and tuning the N-core of the hexaphyrin aiming at bimetallic complexes. The larger β-cyclodextrin unit was selectively functionalized with aldehyde linkers on its primary rim which were further reacted with 2 eq. of pentafluorophenyl tripyrrane in acidic conditions, followed by DDQ oxidation. Doubly-linked HCD hybrids were obtained with structural variations in the hexaphyrin macrocycles depending on the MSA concentration (2 vs 200 mM) producing either regular ([26]rectangular/[28]Möbius) or doubly N-confused dioxo ([26]rectangular) scaffolds. For the latter, two isomers were isolated featuring mirror transoid skeletons and long-side meso-linking patterns, giving rise to planar chirality at the origin of intense and opposite electronic circular dichroism (ECD) spectra. Zn(II) complexation was then investigated leading to two main findings. (i) The regular [28]Möbius HCD afforded a mixture of monometallic Möbius Zn(II) complexes in the presence of acac ligand. ECD spectroscopy indicated a chirality transfer from the β-cyclodextrin favoring a *P* Möbius twist, but opposite to that arising from the narrower α-cyclodextrin congener (*M* twist favored). (ii) Owing to N_3O coordination boxes, dissymmetric bimetallic Zn(II) complexes were readily formed with the doubly N-confused dioxo HCDs through a positive cooperative process. Both metal centers bind a DMAP ligand in axial positions, which is of interest for the further engineering of novel ditopic chiral metalloreceptors.

KEYWORDS: Hexaphyrin, Cyclodextrin, Conformation, Aromaticity, Möbius, N-confused

*Correspondence to: mickael.menand@sorbonne-universite.fr, stephane.legac@univ-rennes1.fr

INTRODUCTION

In the last two decades, stimulated by the facile one-pot synthesis of a series of *meso*-aryl expanded porphyrins by Osuka and coworkers[1], the flourishing chemistry of azaannulenic systems larger than porphyrins has witnessed an ever-growing diversity of scaffolds. Beyond β- and *meso*-functionalization, isomeric, core-modified, fused, π-extended, twisted, among other types of congeners, afford a huge set of possibilities for the emergence of novel π-functional systems[2]. Besides, conformational flexibility, coordination/organometallic chemistry, aromaticity, inherent chirality, are key interlinked features of expanded porphyrins. Orchestrating these features with appropriate external stimuli opens the way to ever-complex adaptive systems.

Until recently, a particular domain of engineering consisting in the coupling of an expanded porphyrin with an hydrophobic cavity has remained under-explored. Considering the previous work achieved with porphyrin-cyclodextrin conjugates bringing selectivity in molecular recognition and catalysis[3], the emergence of novel properties was expected to arise from the controlled association of larger porphyrin congeners with such cavities. With this idea in mind, the covalent assembly of hexaphyrin and α-cyclodextrin subunits was recently developed by our groups leading to the so-called family of hexaphyrin-cyclodextrin hybrids (Figure 1)[4]. Initially, the regular hexaphyrin scaffold was connected by three linkers to a single α-cyclodextrin or by six linkers to two α-cyclodextrins (capped *vs* sandwiched architectures). Recently, more accessible compounds exhibiting two linkers between the subunits were designed. Combining the specific properties of these two families of macrocycles led indeed to unique features with a high degree of control allowing, for instance, to switch over (anti)aromatic configurations through redox processes[4a], tune the communication between both platforms through temperature control[4b,c], and even orchestrate subtle chiral communications throughout the hole hybrid to ultimately control the torsion preference of a Möbius strip[4d].

In the present contribution, we were interested in increasing the diversity of HCD compounds following two main directions: enlarging the confined space provided by the cyclodextrin and tuning the N-core of the hexaphyrin aiming at bimetallic complexes. We logically turned our attention towards the β-cyclodextrin (β-CD) having one more glucose unit compared to the α-CD. In addition to a larger cavity, the di-functionalization of the β-CD produces C_1-symmetrical species which increases the global dissymmetry of the targeted hybrids.

<Figure 1>

RESULTS AND DISCUSSION

1. Synthesis

The synthesis of the targeted HCDs was attempted following the same strategy as that used with the α-cyclodextrin based ones (Scheme 1)[4d]. Briefly, the commercial β-cyclodextrin was engaged in a two-step sequence consisting of the per-benzylation of the alcohol functions followed by a selective de-*O*-benzylation of the A,D-positions of the primary rim[5]. Compound **3** was isolated in good yield (70%) on a large scale. Subsequent functionalization with acetal-protected linker **4** led to compound **5** after chromatography purification (99 % yield), and treatment with TFA led to the bis-aldehyde cyclodextrin **6** without further purification (61% yield). Compound **6** was then engaged in an acid catalyzed [2+1] macrocyclisation reaction with tripyrrane **7**, followed by DDQ oxidation. In standard conditions (*i.e.* 33 mM in CH_2Cl_2 with 2 mM methanesulfonic acid [MSA]),[6] the expected hybrids were readily formed and isolated in moderate yield. As discussed

below, two regular HCDs were characterized, namely the oxidized form **[26]1** exhibiting a rectangular conformation (4 %) and the reduced form **[28]1** consisting of a dynamic mixture of rectangular and Möbius conformations (6 %). Surprisingly, the reaction proceeded differently with a large excess of acid (*ca.* 200 mM of MSA instead of 2 mM). Indeed, using these harsher conditions, we were able to obtain directly two doubly N-confused dioxo hybrids in a one-pot process. The corresponding compounds **[26]2a** and **[26]2b** were isolated in low but fully reproducible 1.4 and 1.1 % yields, respectively (Scheme 1). The conformational analysis (*vide infra*) revealed a rectangular conformation for both hybrids with mirror transoid skeletons and meso-linking patterns (Scheme 1). It is noteworthy that several colored bands were isolated during the purification process, meaning that other HCDs of potential interest may be formed, these will be reported in due time. Attempts to improve the yield of the doubly N-confused dioxo products remained unfruitful. However, some interesting highlights can be drawn from these attempts and their qualitative analyses (Matrix Assisted Laser Desorption Ionization [Maldi] spectra and TLC profiles):

(i) Using the narrower α-cyclodextrin bis-aldehyde congener[4d] instead of **6** did not afford any compounds of interest. This suggests that the β-cyclodextrin introduces specific constraints during the macrocyclization process providing a more favorable degree of preorganization.

(ii) Tuning the MSA concentration orients the outcome : *low* concentrations (2-20 mM) afford only the regular hexaphyrins; an *intermediate* one (100 mM) affords a mixture of both scaffolds; and *high* concentrations (200-300 mM) lead only to the doubly N-confused dioxohexaphyrins.

(iii) The doubly N-confused dioxo products rapidly form, being observed within 5 min after the addition of MSA (200 mM);

(iv) Starting the reaction at low MSA concentration (2 mM for 30 min) to form the hexaphyrinogen intermediate(s) and increasing the concentration of MSA (200 mM) led to a similar result as the direct introduction of excess of MSA. This suggests that the confusion might operate on hexaphyrinogen intermediate(s).

Following the independent discovery of N-confused porphyrins by the groups of Furuta[7] and Latos-Grażyński[8] in 1994, Lindsey and coworkers improved the synthesis of this porphyrinoid five years later and, in their seminal paper, questioned the unique role of MSA in the “confusion” process[9]. Here also, the formation of the confused products is conditioned by large concentrations of MSA which raises many questions that are awaiting further experiments. To the best of our knowledge, until now, the preparation of doubly N-confused dioxohexaphyrins has been restricted to two different approaches, *i.e.* starting from a N-confused tripyrrane[10] or through a copper-mediated rearrangement of a regular hexaphyrin[11]. This particular scaffold has been largely investigated by the group of Furuta and co-workers[12-17] and, in contrast to the regular hexaphyrin skeleton, exhibits remarkable and predictable coordination properties affording bimetallic complexes of interest in sensing phenomena, optoelectronic and magnetic applications, especially in the near-infrared window[10,11,16a,18]. The covalent capping of a macrocyclic host by a doubly N-confused dioxohexaphyrin is unprecedented, the newly formed HCD hybrids thus fully deserve to be investigated.

<Scheme 1>

2. UV-vis absorption, NMR characterization and conformational study

The four new HCDs of Scheme 1 were characterized by HRMS, 2D NMR, UV-vis absorption and ECD spectroscopies. Their 26π or 28π oxidation states as well as the doubly N-confused dioxo scaffolds, were deduced from HRMS analysis (Supporting Information, SI). **[26]1** displays a deep purple color in solution, and exhibits a UV-vis absorption spectrum in

agreement with an aromatic character, with a sharp intense Soret-like band at 576 nm and four Q-like bands spanning 730-1020 nm (Figure 2c, red curve). Its ^{1}H NMR displays a well-defined C_1 dissymmetric pattern characteristic of a rectangular aromatic conformation (diatropic ring current), with four inner β-pyrrolic protons in the shielded region (-2.65 to -3.15 ppm) and eight outer ones deshielded (9.02 to 9.32 ppm) (Figure 3b). Two inner NH protons are shielded as well (-1.87 and -1.66 ppm) whereas the two meso-phenyl rings linked to the cyclodextrin experience a downfield shift in agreement with their peripheral positions. The linking pattern was further assessed by NOE correlations between ArH-*ortho* and two β-CH from two different outer pyrroles. These correlations are in accordance with a *meso*-linking pattern located on the short sides of the rectangle. In addition, through-space correlations between two *ortho*-fluorine atoms of adjacent penta-fluorophenyl groups attest their location on the long-sides of the hexaphyrin (SI). Besides, two benzyl units are shielded (δH_{para} = 5.89/3.98 ppm) and occupy the confined space between the hexaphyrin and the cyclodextrin. All these features are shared by the α-cyclodextrin hybrid counterpart[4d], but the behavior of the cyclodextrin torus differs for the β-one for which a broadening of two glucose units is observed which sharpen upon heating (SI). This suggests a higher constraint in the bridge which is more favorably assumed by the flexible cyclodextrin part rather than the more rigid hexaphyrin part.

<Figure 2>

<Figure 3>

In contrast, **[28]1** displays a blue-violet color in solution and exhibits a UV-vis absorption spectrum combining aromatic and antiaromatic absorption contributions, as deduced from comparison with reference compounds **[28]8** (Möbius aromatic)[19] and **[28]9** (Hückel antiaromatic)[4a] (Chart 1, Figure 2c, blue curve and inset). Indeed, the spectrum shows on one hand maxima at 602 (Soret-like), 770, 863, ~890 and ~1015 nm (Q-like), in agreement with a Möbius aromatic character, and on the other hand maxima at 490 and ~565 nm accompanied with a broad and weak absorption spanning 700-1100 nm, in agreement with a Hückel antiaromatic character. Besides, the ^{1}H NMR of **[28]1** is broad and ill-defined at 300K, which is consistent with a mixture of conformationally flexible compounds. At low temperature (below 263K), a new broad signature appeared (Figure 3a inset and SI) with deshielded resonances, *i.e.* two signals at 24.6 and 26.1 ppm and four ones in the 18-21 ppm region. From comparison with the triply-linked hybrid **[28]9** (Chart 1)[4a], these signals are consistent with respectively two inner NH and four inner β-pyrrolic protons of a rectangular antiaromatic conformation. Both UV-vis and NMR analyses indicate that **[28]1** consists in a dynamic mixture of Möbius aromatic and rectangular antiaromatic conformations, namely **[28]1-M** and **[28]1-R** (Scheme 1). This equilibrium contrasts with the behavior of the α-cyclodextrin congener (**[28]10**, Chart 1) adopting a clear preference towards the Möbius aromatic form into which the unstable Hückel antiaromatic totally converts[4d]. While the interplay between both platforms is clearly influenced by the size of the cavity, a fine understanding of the mechanical constraints acting on the Möbius-rectangular equilibrium remains to be tackled. Oxidation of the mixture gave further insights on the *meso* substitution pattern. Indeed, addition of DDQ to **[28]1** led to the formation of the short-side linked **[26]1** (minor product) and a mixture of rectangular [26]hexaphyrins (major products) with *a fortiori* long-side linking patterns[20]. This mixture was fully converted to **[26]1** upon heating at 50 °C for 1h. In line with the α-cyclodextrin congeners **[28]10** (Chart 1)[4d], this behavior is consistent with **[28]1** exhibiting predominantly (if not exclusively) long-side *meso* substitution pattern(s), the corresponding oxidized form(s) evolving through pyrrole isomerization[21][4d] to the thermodynamic product **[26]1** functionalized on its short sides.

<Chart 1>

Concerning the doubly *N*-confused dioxo **[26]2a** and **[26]2b**, their UV-vis absorption spectra match with the literature with notably an intense Soret-like band at 574 nm, a shoulder at 597 nm and four Q-like bands at 730, 800, 914 and 1055 nm[10b,11], indicating a 26π aromatic feature (Figure 2d). Both compounds exhibit well-defined dissymmetric ^{1}H NMR spectra evidencing a diatropic ring current with a clear splitting of the 10 *peripheral* β-CH protons (9.10 to 11 ppm region) and the 4 *inner* located NH protons (-0.70 to -1.50 ppm region) (Figure 3c,d). More specifically, for each isomer *i.e.* **[26]2a** (/**[26]2b**), the β-CH of the two confused pyrroles resonate at 10.92(/10.94) and 10.89(/10.90) ppm, and their corresponding inner NH at -1.12(/-1.16) and -1.39(/-1.46) ppm. 2D NMR analysis (COSY, ROESY, Figure 4b,c) allowed us to discriminate between the twelve possible doubly N-confused dioxo structures that could match with such a pattern (six "transoid" and six "cisoid")[10b]. Indeed, for each of the three possible linking patterns (one short-side and two long-sides), there are four possible arrangements of the confused pyrroles depending on the C=O orientations, whether they are adjacent to the *meso*-aryl linker or to the C_6F_5 (Chart 2). First, NH and β-CH of each pyrrole were identified through COSY correlations. Then, ROESY of both compounds showed NOE correlations between *ortho*-proton of the *meso*-aryl linkers and β-CH of the confused pyrroles indicating that the linking patterns correspond to the long-side and not the short-side one. Finally, inner NH of normal and confused pyrroles correlate two-by-two (Figure 4a) defining a "transoid" orientation of both C=O functions, that are adjacent to the *meso* aryl linkers. Consequently, the two isomers with N_3O coordination boxes can only exhibit opposite long-side linking patterns, each being associated to a single transoid-confusion pattern as drawn in Figure 4a. It is noteworthy that isomers **[26]2a** and **[26]2b** correspond to an identical doubly N-confused dioxo scaffold bridged on one or the other side by the cyclodextrin.

<Chart 2>

<Figure 4>

Apart from the cyclodextrin chirality, the long-side bridging of the hexaphyrin generates planar chirality,[4d] **[26]2a** and **[26]2b** exhibiting mirror transoid skeletons and linking patterns (Scheme 1). Interestingly, these two diastereomers display intense and quasi-mirror ECD spectra with bisignate Cotton effect in the Soret wavelength region, weakly influenced by the cyclodextrin's chirality (Figure 2b). In comparison, the ECD spectra of the regular hybrids **[28]1** and **[26]1** revealed only weak signals (Figure 2a). These remarkable and unexpected ECD signatures of the doubly N-confused dioxo scaffolds compare with the topologically chiral π-systems of Möbius and Figure 8 porphyrinoids[22], suggesting that the π-systems of **[26]2a** and **[26]2b** experience strong and opposite deformations. More investigations are required to decipher these chiroptical properties.

3. Zn(II) metalation

<Figure 5>

The Zn(II) complexation behavior of the new HCD hybrids was evaluated by ^{1}H NMR studies. Concerning **[28]1**, a behavior similar to its α-cyclodextrin congener **[28]10** was observed[4d]. In $CDCl_3/CD_3OD$ mixture, addition of $Zn(OTf)_2$ had no effect on the NMR spectrum, but subsequent addition of acetylacetone (acac) ligand afforded instantaneously a set of four Möbius 'Zn(acac)' complexes in *ca.* 3:2.5:1:0.5 ratio (Figure 5a,b) consistent with a mixture of two *P*-twisted and two *M*-twisted isomers as described below. The Möbius aromatic rings, frozen on the NMR time scale, display three characteristic sets of β-CH signals resulting from their diatropic ring current: *inner* (-1.3 to -2.9 ppm), *twisted* (4.85 to 4.35 ppm) and *outer*

(8.3-7.0 ppm). The acac ligands are bound in a slow exchange process at 298 K, one of the two methyl groups being strongly shielded at *ca.* δ = -1.1 ppm (Figure 5b). This is consistent with a 'Znacac' moiety bound to a dipyrrin site involving the *twisted* pyrrole and a tetrahedral coordination geometry for the Zn(II) ion orienting the two acac methyl groups *towards* and *outwards* the Möbius ring (Figure 5a)[4d][23]. In our previous work[4d], the Möbius complex of **[28]10** behaved as a totem of three types of chirality (*i.e.* central [cyclodextrin, fix], planar [meso-pattern, dynamic] and Möbius [dynamic] chirality), featuring multiple intramolecular transfers of chirality tuned by coordination and ultimately acting on the *P*/*M* Möbius selectivity. Briefly, we found that a single Möbius twist (over four possible ones, see SI) corresponds to a given long-side *meso*-linking pattern, owing to a highly selective planar-to-Möbius transfer of chirality, whereas the chirality of the cyclodextrin discriminated the two long-side *meso*-linking patterns (central-to-planar transfer of chirality). Herein, the mixture of four Möbius complexes likely arises from a similar stereoselective scheme: (i) the two major and two minor complexes (blue/red triangles) correspond to isomers featuring opposite long-side linking patterns discriminated by the cyclodextrin (central-to-planar transfer of chirality); (ii) for a given long-side linking pattern, the twist can be located on the occlusive (2 glucose units) or the aversive (3 glucose units) side of the bridge with moderate selectivity (3:2.5 ratio and 1:0.5 ratio), nonetheless with a high selectivity for a single Möbius twist (over the four possible ones) for each of these possibilities (planar-to-Möbius transfer of chirality)[4d]. More detailed investigations are needed to substantiate this hypothesis. All in all, ECD analysis revealed a positive bisignate Cotton effect in the Soret region upon addition of the acac ligand, supporting a global chirality induction favoring the *P* twist (Figure 5c, blue curve)[24]. This stereoselectivity contrasts with the α-cyclodextrin congener **[28]10** leading to *M* twist amplification in the same metalation conditions (Figure 5c, dashed line)[4d]. Hence, tuning the size of the cavity of the hybrids allows to ultimately invert the π-system twisting preference. It yet remains unclear how the mechanical stresses apply to discriminate the opposite meso-linking patterns.

<Figure 6>

In parallel, we further investigated Zn(II) complexation with the native form of the oxidized **[26]1** hybrid. However, despite our efforts to cover various conditions, we were unable to coordinate Zn(II) ion within this regular hexaphyrin consistently with the previous work of Osuka and coworkers[25]. In contrast, the N_3O boxes of **[26]2a** and **[26]2b** allowed Zn(II) insertion and formation of the corresponding bimetallic complexes **[26]2a•Zn$_2$** and **[26]2b•Zn$_2$** (Figure 6a, confirmed by HRMS analysis), in accordance with the previous work of Furuta and co-workers[10a,11,18b]. The monitoring of the metalation reaction (^{1}H NMR, DMSO-d_6 at 80 °C) revealed a full completion within 3 hours with a cooperative coordination process (Figure 6b,c). Indeed, the final bimetallic complexes were observed as major products at any stage of the metalation together with traces of transient patterns attributed to putative monometallic complexes. After precipitation with water, the isolated complexes in $CDCl_3$ likely correspond to aqua species featuring five-coordinate zinc centers. The residual broad water signal is shielded by *ca.* -0.5 ppm ($\delta \approx 1$ ppm) which is consistent with a fast exchange process on the NMR time scale. An X-ray structure of a bis Zn(II)-aqua complex of the benchmark doubly N-confused dioxo **[26]11** (Chart 1) was reported by Furuta and co-workers[18b], revealing slight opposite out-of-plane displacements of the zinc centers, the aqua axial ligands being located on opposite sides of the macrocycle (*trans* coordination). In the case of **[26]2a•Zn$_2$[H$_2$O]$_2$** and **[26]2b•Zn$_2$[H$_2$O]$_2$**, a similar *trans* coordination geometry would orient the zinc axial ligands *towards* and *away from* the cyclodextrin[26]. We finally explored their coordination behavior, adding an excess of 4-(dimethylamino)pyridine (DMAP) to both complexes. In each case, the new ^{1}H NMR pattern was accompanied by a downfield shift of the residual water signal, indicating a release of the coordinated water. Besides, the DMAP resonances were broaden at room temperature in line with an intermediate

exchange process on the NMR time scale. Slowing down the exchange process (VT NMR down to 183 K in CD_2Cl_2 with **[26]2b•Zn$_2$[DMAP]$_2$**) revealed two different complexes in a *ca.* 2:1 ratio, with a total coordination of four different DMAP molecules as deduced from a 2D ROESY experiment (SI). Aromatic protons of the bound DMAP ligands experience a strong shielding ($\Delta\delta$ up to -7 ppm, Figure 6a, inset), attesting their axial coordination to zinc. Yet, the ill-defined NMR patterns at low temperature do not allow assessing the orientations of the DMAP ligands. One plausible explanation would be the formation of two *trans* complexes with *inward*/*outward* axial DMAP ligands bound to one or the other non-equivalent zinc centers of the bimetallic complexes, with moderate selectivity, as drawn in Figure 6a[27]. Although further investigations are required to substantiate this hypothesis, this last observation is stimulating for the engineering of novel chiral ditopic metalloreceptors that could find applications in sensing and catalysis.

CONCLUSION

In conclusion, we have successfully extended the family of hexaphyrin-cyclodextrin hybrids by increasing the size of the cyclodextrin unit by one glucose unit, and by modifying the hexaphyrin scaffold from regular to doubly N-confused dioxo. The enlarged cavity of the β-cyclodextrin based hybrids leads to contrasting differences in stability (antiaromatic contribution) and chirality (opposite twisting) preferences compared to the narrower α-cyclodextrin counterparts. Combining both the enlargement and the confusion modifications leads to chiral expanded porphyrins with two different N_3O coordination sites, readily forming bimetallic Zn(II)-DMAP complexes. To further take advantage of the confined space of the hybrids, it now becomes essential (i) to determine the degree of coupling between the coordination boxes and the cyclodextrin's cavity, *e.g.* as a function of the linking pattern(s) (planar stereoisomerism); (ii) to access heterobimetallic complexes; (iii) to get water-soluble hybrids. Work along these lines are underway in our laboratories.

Acknowledgements

We are grateful to the Agence Nationale de la Recherche for financial support (ANR research program PRALLOCAT, ANR-16-CE07-0014 and MIXAR, ANR-20-CE07-0026).

Supporting information

Full experimental details and NMR spectra are given in the supplementary material. This material is available at http://www.u-bourgogne.fr/jpp/.

REFERENCES

1. Shin J-Y, Furuta H, Yoza K, Igarashi S and Osuka A. *J. Am. Chem. Soc*. 2001; **123**: 7190-7191.
2. Selected reviews covering the field of expanded porphyrins: a) Sessler JL and Seidel D. *Angew. Chem. Int. Ed*. 2003; **42**: 5134-5175. b) Yoon ZS, Osuka A and Kim D. *Nat. Chem*. 2009; **1**: 113-122. c) Shin J-Y, Kim KS, Yoon M-C, Lim JM, Yoon ZS, Osuka A and Kim D. *Chem. Soc. Rev*. 2010; **39**: 2751-2767. d) Stępień M, Sprutta N and Latos-Grażyński L. *Angew. Chem. Int. Ed*. 2011; **50**: 4288-4340. e) Saito S and Osuka A. *Angew. Chem. Int. Ed*. 2011; **50**: 4342-4373. f) Osuka A and Saito S. *Chem. Commun*. 2011; **47**: 4330-4339. g) Roznyatovskiy VV, Leeb C-H and Sessler JL *Chem. Soc. Rev*. 2013; **42**: 1921-1933. h) Tanaka T and Osuka A. *Chem. Rev*. 2017; **117**: 2584-2640. i) Mo Sung Y, Oh J, Cha W-Y, Kim W, Min Lim J, Yoon M-C and Kim D. *Chem. Rev*. 2017; **117**: 2257-2312. j) Szyszko B, Białek MJ,

Pacholska-Dudziak E and Latos-Grażyński L. *Chem. Rev*. 2017; **117**: 2839-2909. k) Sarma T and Panda PK. *Chem. Rev*. 2017; **117**: 2785-2838. l) Chatterjee T, Srinivasan A, Ravikanth M and Chandrashekar TK. *Chem. Rev*. 2017; **117**: 3329-3376. m) Reddy BK, Basavarajappa A, Ambhore MD and Anand VG. *Chem. Rev*. 2017; **117**: 3420-3443.

3. For recent reviews dealing with porphyrin-cyclodextrin conjugates, see : a) Vonesch M, Wytko JA, Kitagishi H, Kano K and Weiss J. *Chem. Commun*. 2019; **55**: 14558-14565. b) Li, F-Q, Chen Y and Liu Y. In *Handbook of Macrocyclic Supramolecular Assembly*; Liu Y, Chen Y and Zhang H-Y, Eds.; Springer, Singapore, 2020; pp 1073–1104. For early work, see: c) Kuroda Y, Hiroshige T, Sera T and Ogoshi H. *Carbohydr. Res*. 1989; **192**: 347-350. d) Kuroda Y, Hiroshige T, Sera T, Shiroiwa Y, Tanaka H and Ogoshi H. *J. Am. Chem. Soc*. 1989; **111**: 1912-1913.
4. a) Ménand M, Sollogoub M, Boitrel B and Le Gac S. *Angew. Chem. Int. Ed*. 2016; **55**: 297-301. b) Le Gac S, Boitrel B, Sollogoub M and Ménand M. *Chem. Commun*. 2016; **52**: 9347-9350. c) Ménand M, Sollogoub M, Boitrel B and Le Gac S. *Chem. Eur. J*. 2018; **24**: 5804-5812. d) Benchouaia R, Cissé N, Boitrel B, Sollogoub M, Le Gac S and Ménand M. *J. Am. Chem. Soc*. 2019; **141**: 11583-11593.
5. a) Pearce AJ and Sinaÿ P. *Angew. Chem. Int. Ed*. 2000; **39**: 3610-3612. b) Lecourt T, Herault A, Pearce AJ, Sollogoub M and Sinaÿ P. *Chem. Eur. J*. 2004; **10**: 2960-2971.
6. Suzuki M and Osuka A. *Org. Lett*. 2003; **5**: 3943-3946.
7. Furuta H, Asano T and Ogawa T. *J. Am. Chem. Soc*. 1994; **116**: 767-768.
8. Chmielewski PJ, Latos-Grazynski L, Rachlewicz K and Glowiak T. *Angew. Chem., Int. Ed*. 1994; **33**: 779-781.
9. a) Geier GR III, Haynes DM and Lindsey JS. *Org. Lett*. 1999; **1**: 1455-1458. b) See also: Fisher JM, Kensy VK and Geier GR III. *J. Org. Chem*. 2017; **82**: 4429-4434.
10. a) Srinivasan A, Ishizuka T, Osuka A and Furuta H. *J. Am. Chem. Soc*. 2003; **125**: 878-879. b) Shimomura K, Kai H, Nakamura Y, Hong Y, Mori S, Miki K, Ohe K, Notsuka Y, Yamaoka Y, Ishida M, Kim D and Furuta H. *J. Am. Chem. Soc*. 2020; **142**: 4429-4437.
11. Suzuki M, Yoon M-C, Kim DY, Kwon JH, Furuta H, Kim D and Osuka A. *Chem. Eur. J*. 2006; **12**: 1754-1759.
12. For reviews, see: a) Srinivasan A and Furuta H. *Acc. Chem. Res.* 2005; **38**: 10-20. b) Toganoh M and Furuta H. *Chem. Commun*. 2012; **48**: 937-954.
13. For doubly N-confused hexaphyrin π-radicals, see: Hisamune Y, Nishimura K, Isakari K, Ishida M, Mori S, Karasawa S, Kato T, Lee S, Kim D and Furuta H. *Angew. Chem. Int. Ed*. 2015; **54**: 7323-7327.
14. For singly N-confused hexaphyrins, see: a) Gokulnath S, Yamaguchi K, Toganoh M, Mori S, Uno H and Furuta H. *Angew. Chem. Int. Ed*. 2011; **50**: 2302-2306. b) Gokulnath S, Toganoh M, Yamaguchi K, Mori S, Uno H and Furuta H. *Dalton Trans*. 2012; **41**: 6283-6290.
15. For triply N-confused hexaphyrins, see: Xie Y-S, Yamaguchi K, Toganoh M, Uno H, Suzuki M, Mori S, Saito S, Osuka A and Furuta H. *Angew. Chem. Int. Ed*. 2009; **48**: 5496-5499.
16. For photophysical properties of N-confused hexaphyrins, see: a) Kwon JH, Ahn TK, Yoon M-C, Kim DY, Koh MK, Kim D, Furuta H, Suzuki M and Osuka A. *J. Phys. Chem. B* 2006; **110**: 11683-11690. b) Ryu J-H, Nagamura T, Nagai Y, Matsumoto R, Furuta H and Nakamura K. *Mol. Cryst. Liq. Cryst*. 2006; **445**: 249-257. c) Ryu J-H, Ito F, Nagamura T, Nakamura K, Furuta H, Shibata Y and Itoh S. *Chem. Phys. Lett.* 2007; **443**: 274-279. d) Lim JM, Lee JS, Chung HW, Bahng HW, Yamaguchi K, Toganoh M, Furuta H and Kim D. *Chem. Commun*. 2010; **46**: 4357-4359.
17. For theoretical study on conformations of N-confused hexaphyrins, see: a) Toganoh M and Furuta H. *J. Org. Chem*. 2010; **75**: 8213-8223. b) Toganoh M and Furuta H. *J. Org. Chem*. 2013; **78**: 9317-9327.

18. a) Mayer I, Nakamura K, Srinivasan A, Furuta H, Toma HE and Araki K. *J. Porphyrins Phthalocyanines* 2005; **9**: 813-820. b) Ikawa Y, Takeda M, Suzuki M, Osuka A and Furuta H. *Chem. Commun*. 2010; **46**: 5689-5691. c) Ikawa Y, Katsumata S, Sakashita R and Furuta H. *Chem. Lett*. 2014; **43**: 1929-1931. d) Yamasumi K, Nishimura K, Hisamune Y, Nagae Y, Uchiyama T, Kamitani K, Hirai T, Nishibori M, Mori S, Karasawa S, Kato T, Furukawa K, Ishida M and Furuta H. *Chem. Eur. J*. 2017; **23**: 15322-15326. e) Nakazono T and Wada T. *Inorg. Chem*. 2021; **60**: 1284-1288.
19. Sankar J, Mori S, Saito S, Rath H, Suzuki M, Inokuma Y, Shinokubo H, Kim KS, Yoon ZS, Shin J-Y, Lim JM, Matsuzaki Y, Matsushita O, Muranaka A, Kobayashi N, Kim D and Osuka A. *J. Am. Chem. Soc*. 2008; **130**: 13568-13579.
20. These species were not characterized due to short life-time and overlapped (ill-defined) ^{1}H NMR patterns.
21. Suzuki M and Osuka A. *Chem. Commun*. 2005; **29**: 3685-3687.
22. For instance, enantiopur group 10 metal complexes of Möbius **[28]8** exhibit maximum Δδ values ranging (+/-) 200-300 L.mol^{-1}.cm^{-1}, see: Tanaka T, Sugita T, Tokuji S, Saito S and Osuka A. *Angew. Chem. Int. Ed*. 2010; **49**: 6619-6621.
23. For a related structurally characterized Zn(II) coordination geometry, see: Ruffin H, Nyame Mendendy Boussambe G, Roisnel T, Dorcet V, Boitrel B and Le Gac S. *J. Am. Chem. Soc.* 2017; **139**: 13847-13857.
24. The corresponding UV-vis spectrum showed disappearance of the antiaromatic contribution of **[28]1-R**.
25. Mori S, Shimizu S, Shin J-Y and Osuka A. *Inorg. Chem*. 2007; **46**: 4374-4376.
26. The ECD spectra of **[26]2a•Zn$_2$** and **[26]2b•Zn$_2$** are less intense *vs*. the free bases, but still with Cotton effects of opposite signs (SI).
27. The addition of DMAP induces the disappearance of shielded signals of OBn moieties, in agreement with an inward DMAP ligand repelling these OBn moieties away from the confined space between the hexaphyrin and the cyclodextrin.

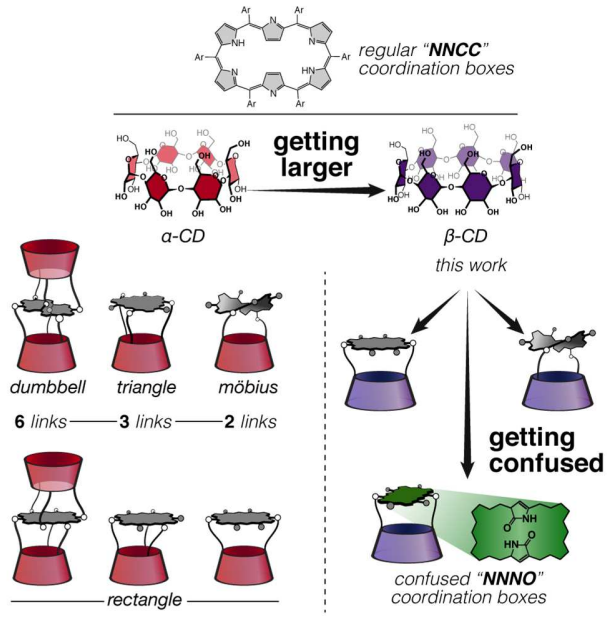

Fig. 1. Left: overview of previously described hexaphyrin-cyclodextrin hybrids, made of a regular hexaphyrin and α-cyclodextrin(s). Right: new HCD hybrids based on a β-cyclodextrin unit doubly linked to a doubly N-confused dioxohexaphyrin (this work).

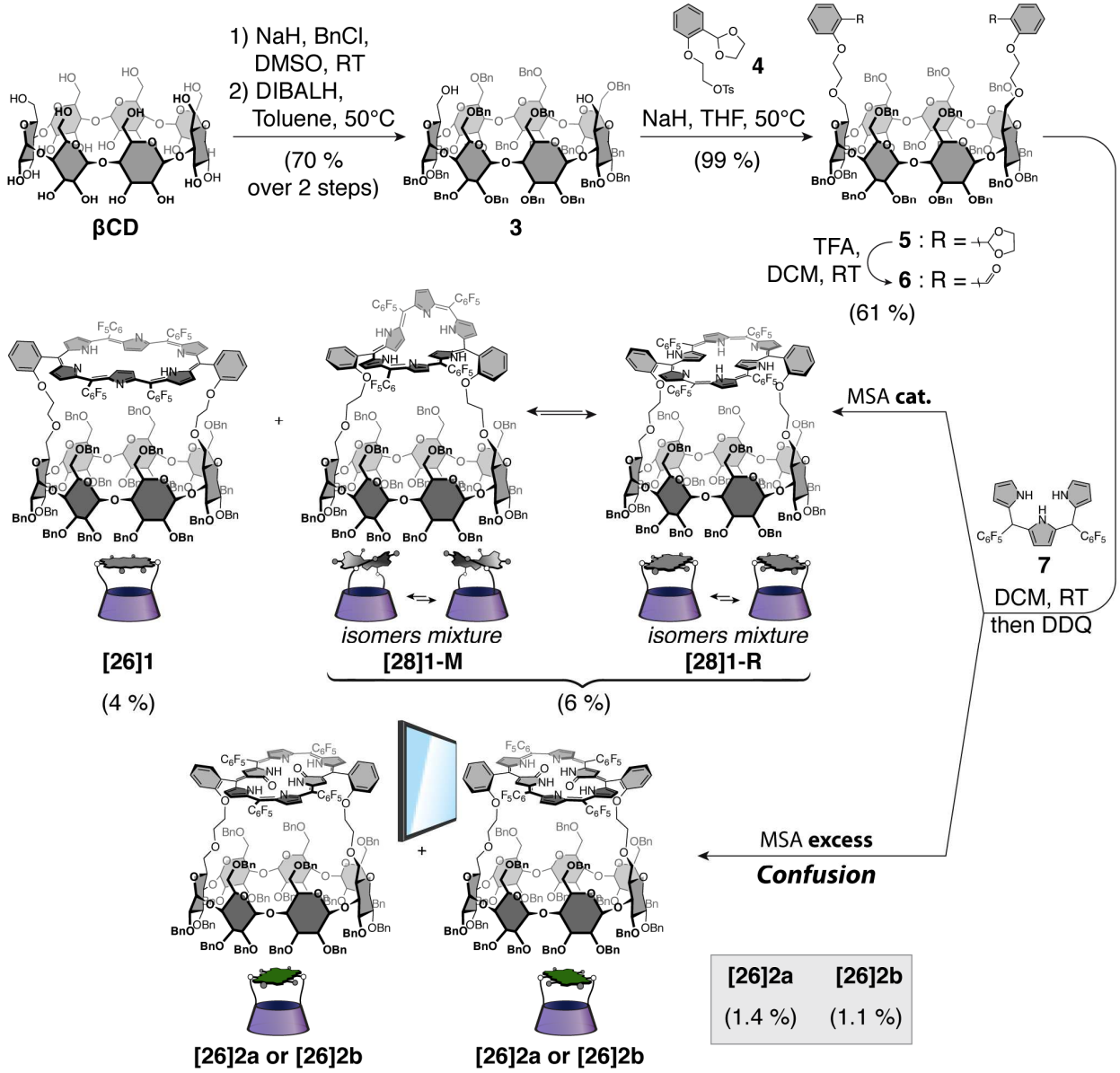

Scheme 1. Synthesis of "regular" vs "doubly N-confused dioxo" HCDs from β-cyclodextrin.

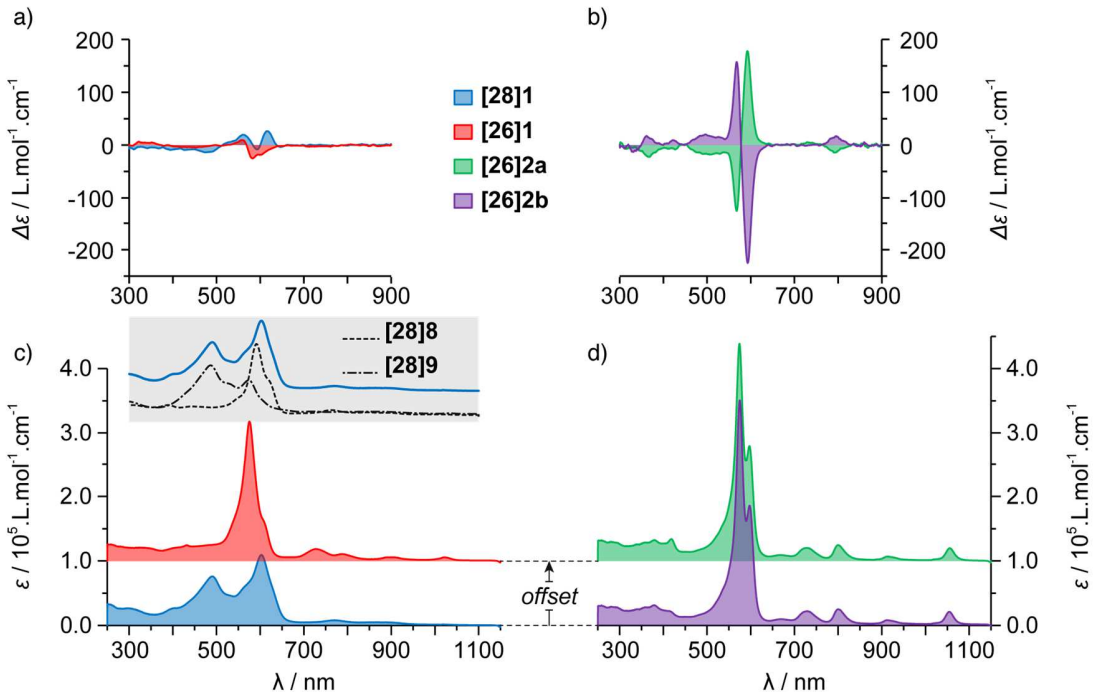

Fig. 2. Electronic circular dichroism (a-b) and UV-vis-NIR absorption spectra (c-d) of **[28]1**, **[26]1**, **[26]2a** and **[26]2b** in $CHCl_3$ (grey inset: comparison between **[28]1**, Möbius aromatic **[28]8** and Hückel antiaromatic **[28]9**).

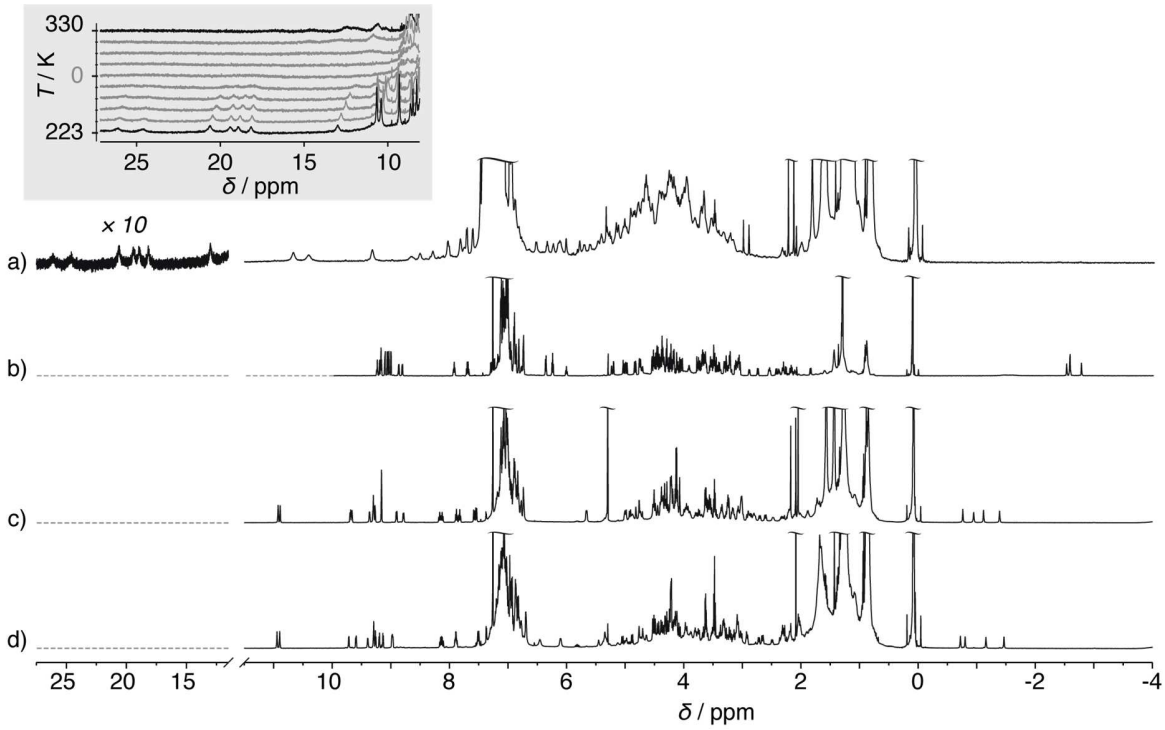

Fig. 3. (a) ^{1}H NMR (500 MHz) of **[28]1** at 223 K in $CDCl_3$ (grey inset : VT-NMR of the deshielded region between 223 and 330 K). (b) ^{1}H NMR (600 MHz) of **[26]1** at 340 K in $CDCl_3$. (c) ^{1}H NMR (500 MHz) of **[26]2a** at 300 K in $CDCl_3$. (d) ^{1}H NMR (500 MHz) of **[26]2b** at 300 K in $CDCl_3$.

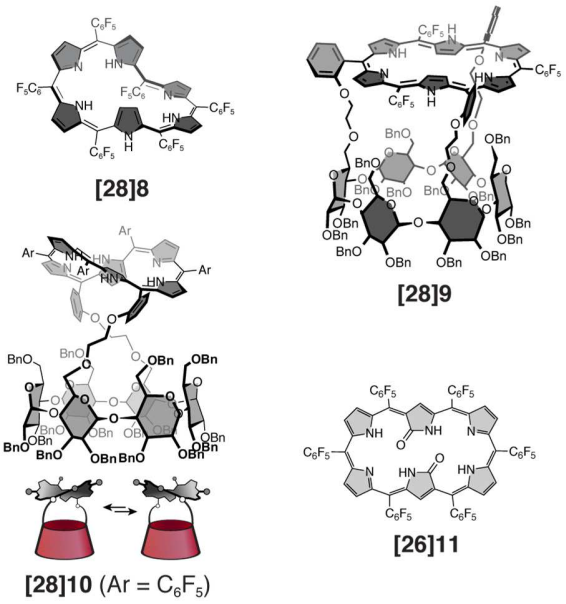

Chart 1. Structures of reference compounds.

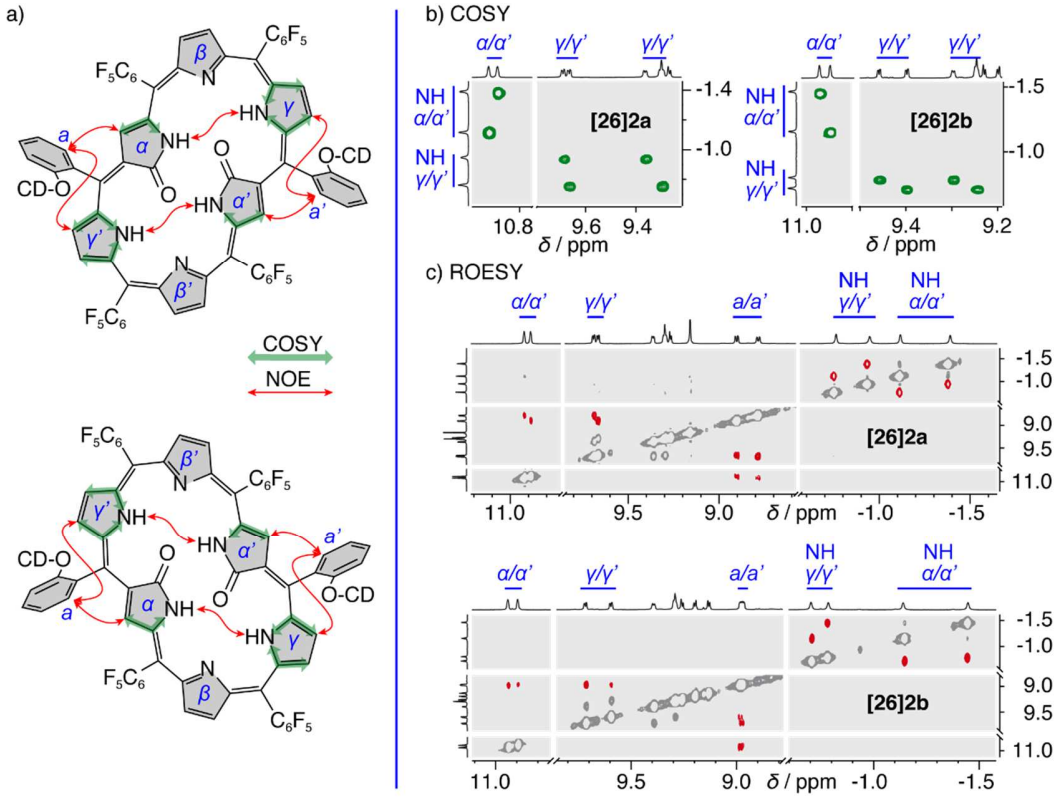

Fig. 4. (a) Selected NOE and COSY correlations indicative of the doubly N-confused dioxo patterns of **[26]2a** and **[26]2b.** (b) COSY spectra of **[26]2a** and **[26]2b** (regions of interest). (c) ROESY spectra of **[26]2a** and **[26]2b** (regions of interest).

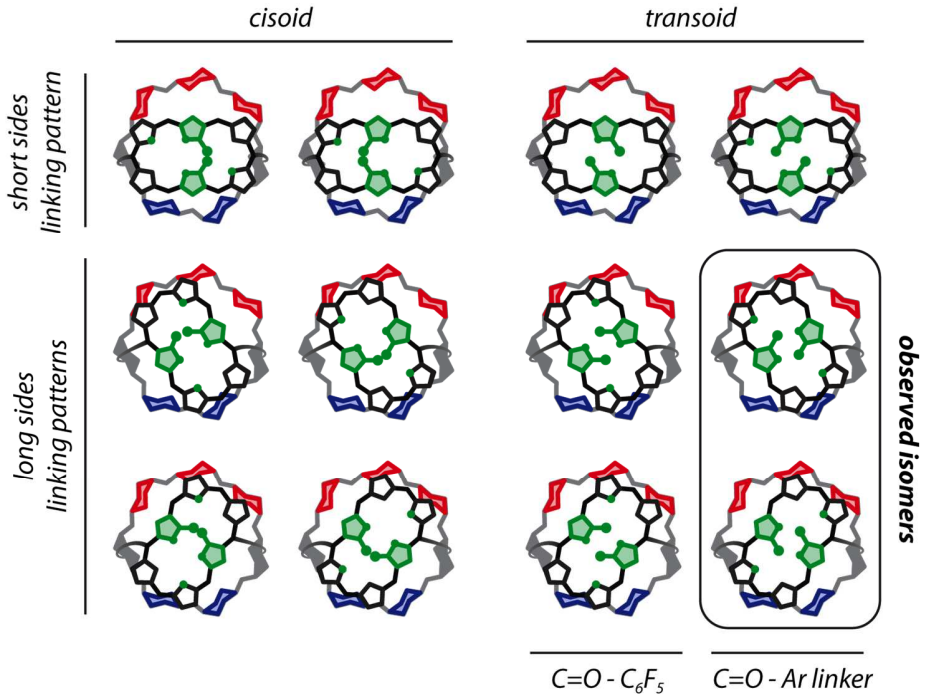

Chart 2. Simplified illustration of the possible isomers for the doubly N-confused dioxo HCDs. The framed illustrations are those observed in the present work.

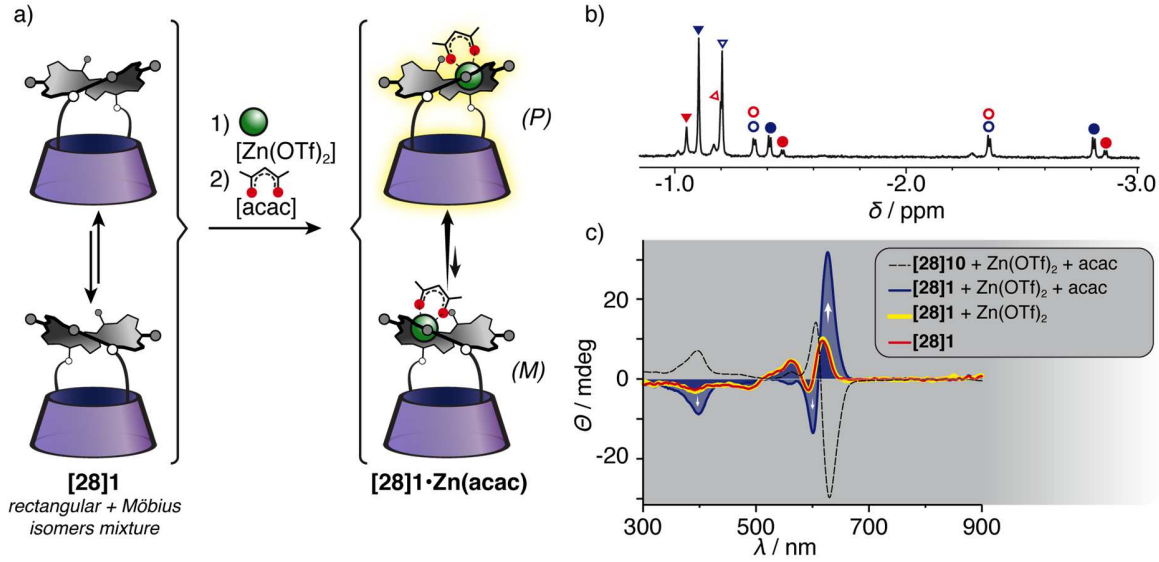

Fig. 5. (a) Metalation scheme of **[28]1** with $Zn(OTf)_2$ and acac in $CDCl_3/CD_3OD$ (9:1) at room temperature. (b) Shielded region of the ^1H NMR spectrum of the metalation (▽,▼,▽,▼: CH_3^{acac} introverted for the four isomers; ○,●,○,● : inner βCH for the four isomers). (c) Electronic circular dichroism spectra of **[28]1** after the sequential addition of $Zn(OTf)_2$ and acac in $CDCl_3/CD_3OD$ (9:1) at room temperature and ECD spectrum **[28]10** metalated in the same conditions (intensity arbitrary scaled)[4d].

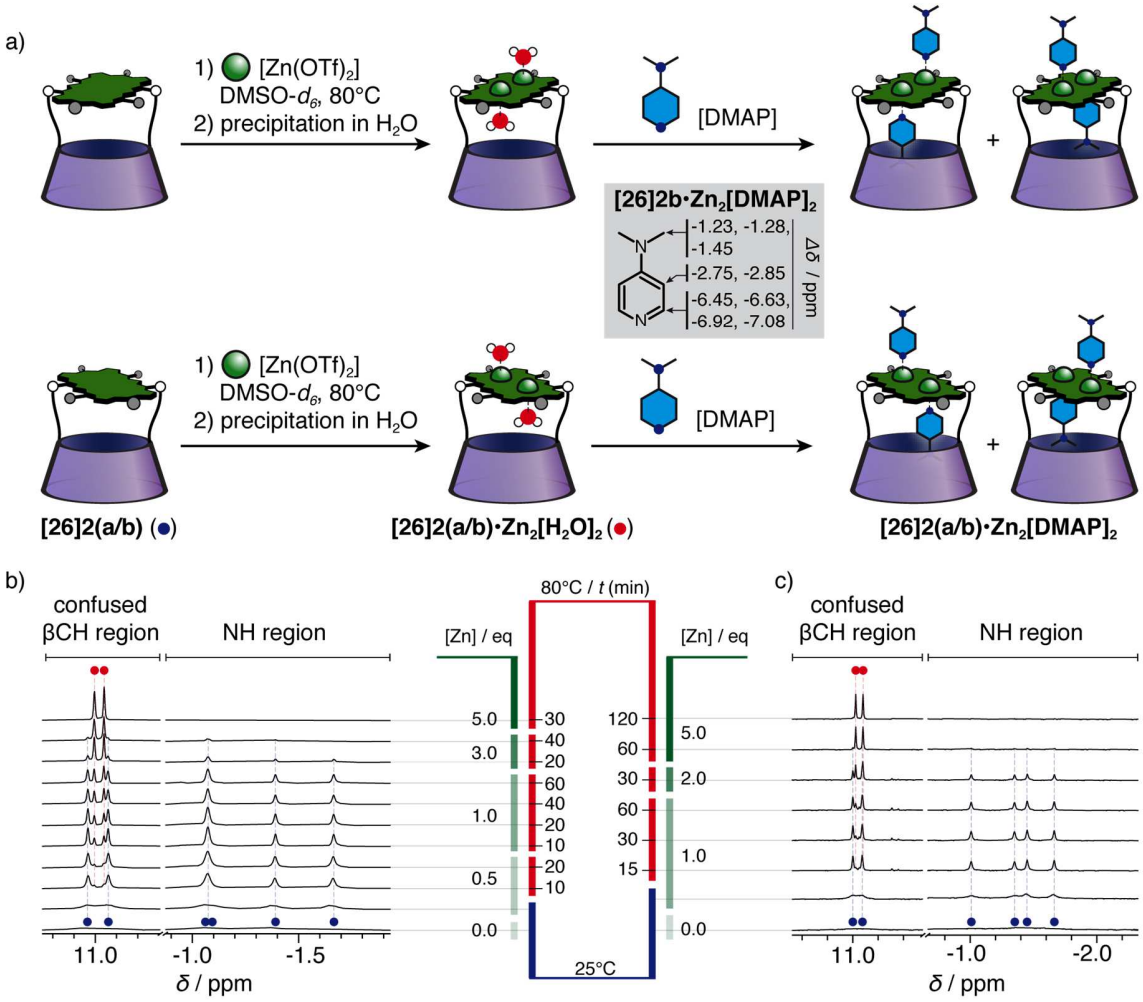

Fig. 6. (a) Metalation scheme of **[26]2a** and **[26]2b** with $Zn(OTf)_2$ in DMSO-d_6 at 80°C, followed by coordination of DMAP in $CDCl_3$ or CD_2Cl_2 at room temperature. (b) Stacked spectra of the ^1H NMR titration (500 MHz, DMSO-d_6, 300K) of **[26]2a** with $Zn(OTf)_2$ (up to 5 equivalents; heating periods at 80°C are indicated for each amount of [Zn]). (c) Stacked spectra of the ^1H NMR titration (500 MHz, DMSO-d_6, 300K) of **[26]2b** with $Zn(OTf)_2$ (up to 5 equivalents; heating periods at 80°C are indicated for each amount of [Zn]). Grey inset: complexation induced shifts (Δδ) of the DMAP protons of **[26]2b•Zn$_2$[DMAP]$_2$** (measured at 210 K in CD_2Cl_2).

Hexaphyrin-cyclodextrin hybrids: getting larger, getting confused

François Robert,[a] Bernard Boitrel,[a] Mickaël Ménand,[b,*] and Stéphane Le Gac [a,*]

Hexaphyrin-cyclodextrin hybrids with an enlarged cavity (β-cyclodextrin) associated to either a regular or a doubly N-confused dioxo hexaphyrin have been synthesized. These two types of modifications have a drastic influence on the chiroptical properties of the hybrids in both Möbius (regular) and planar (confused) conformations, with sign inversions of the circular dichroism spectra. Confused hybrids featuring two different N_3O boxes formed bimetallic Zn(II) complexes enabling the binding of two DMAP molecules in a disymmetric environment.